Published in final edited form as:
J Control Release. 2011 May 10; 151(3): 271–277. doi:10.1016/j.jconrel.2011.01.004.

Nanoscopic Micelle Delivery Improves the Photophysical Properties and Efficacy of Photodynamic Therapy of Protoporphyrin IX

Huiying Ding[†], **Baran D. Sumer**[‡], **Chase W. Kessinger**[†], **Ying Dong**[†], **Gang Huang**[†], **David A. Boothman**[†,#], and **Jinming Gao**[†,*]

[†]Department of Pharmacology, University of Texas Southwestern Medical Center at Dallas, 5323 Harry Hines Boulevard, Dallas, Texas 75390

[#]Laboratory of Molecular Stress Responses, Harold C. Simmons Comprehensive Cancer Center, University of Texas Southwestern Medical Center at Dallas, 5323 Harry Hines Boulevard, Dallas, Texas 75390

[‡]Department of Otolaryngology, Head and Neck Surgery, University of Texas Southwestern Medical Center at Dallas, 5323 Harry Hines Boulevard, Dallas, Texas 75390

Abstract

Nanodelivery systems have shown considerable promise in increasing the solubility and delivery efficiency of hydrophobic photosensitizers for photodynamic therapy (PDT) applications. In this study, we report the preparation and characterization of polymeric micelles that incorporate protoporphyrin IX (PpIX), a potent photosensitizer, using non-covalent encapsulation and covalent conjugation methods. Depending on the incorporation method and PpIX loading percentage, PpIX existed as a monomer, dimer or aggregate in the micelle core. The PpIX state directly affected the fluorescence intensity and $^1O_2$ generation efficiency of the resulting micelles in aqueous solution. Micelles with lower PpIX loading density (e.g. 0.2%) showed brighter fluorescence and higher $^1O_2$ yield than those with higher PpIX loading density (e.g. 4%) in solution. However, PDT efficacy in H2009 lung cancer cells showed an opposite trend. In particular, 4% PpIX-conjugated micelles demonstrated the largest PDT therapeutic window, as indicated by the highest phototoxicity and relatively low dark toxicity. Results from this study contribute to the fundamental understanding of nanoscopic structure-property relationships of micelle-delivered PpIX and establish a viable micelle formulation (i.e. 4% PpIX-conjugated micelles) for *in vivo* evaluation of antitumor efficacy.

Keywords

polymeric micelles; photodynamic therapy; protoporphyrin IX; singlet oxygen; photosensitizer; nanoparticle delivery

[*]Address correspondence to jinming.gao@utsouthwestern.edu.

1. Introduction

Recently, photodynamic therapy (PDT) has received considerable attention as a safe, minimally invasive and tissue selective treatment of cancer and other diseases [1-3]. During PDT, a photosensitizer (PS) drug is first intravenously administered into the patient. Upon light activation at the targeted tissues, singlet oxygen ($^1O_2$) and other reactive oxygen species (ROS) are generated to destroy malignant cells [4,5]. Compared to other therapeutic modalities, PDT is much less invasive than surgery, and is more tumor-selective than chemotherapy and radiotherapy with minimal toxicity to normal tissues. Currently, Photofrin® (porfimer sodium), Visudyne® (verteporfin), Levulan® (5-aminolevulinic acid, 5-ALA) and Metvixia® (methyl aminolevulinic acid) have been approved as PDT drugs by the Food and Drug Administration in the US, and Foscan® (temoporfin) has been approved to treat head and neck cancers in the European Union [3]. Except for 5-ALA, all the other clinically approved PDT drugs are porphyrin-based molecules, which are hydrophobic and have intrinsically low water solubilities. Excipient molecules such as lipid mixtures (e.g. in Visudyne®) and ethanol/poly(propylene glycol) (e.g. in Foscan®) are used to solubilize these agents for intravenous injections. 5-ALA is a pro-drug that can be converted into protoporphyrin IX (PpIX) in rapidly proliferating tumor cells compared to normal tissues leading to selective accumulation of PpIX in tumors [6,7]. The endogenously produced PpIX in turn acts as a potent PS allowing selective destruction of cancer cells. A major disadvantage of this approach is the limited diffusion of 5-ALA through cell membranes because of its polarity. Moreover, it is unstable in aqueous solution from the neutral to basic pH range. In the clinical setting, high doses of 5-ALA must be administered to reach clinically efficacious levels of PpIX. So far, free PpIX cannot be directly injected intravenously due to its low water solubility (~1 μg/mL). Moreover, dark toxicity as well as easy aggregation of PpIX leading to a rapid loss of its ability to generate singlet oxygen further limits the direct clinical use of PpIX [8,9].

Nanoparticles have been developed as an effective PDT drug delivery platform in recent years [10], and extensive research efforts have been devoted to the development of effective nanocarriers for PDT agents including liposomes [11,12], dendrimers [13,14], polymer nanoparticles [15,16] and polymeric micelles [17,18]. Among these, polymeric micelles provide an intriguing option due to their unique core-shell structures in aqueous environment. The hydrophobic core of the micelles provides a naturally compatible environment for loading hydrophobic PS molecules, while the hydrophilic shells stabilize the nanoparticles for increased water solubility and prolong blood circulation. In addition to the solubility enhancement of hydrophobic agents into aqueous solution, micelle encapsulation can also greatly improve the photophysical and photochemical properties of PS in aqueous solution. Singlet oxygen is believed to be the main cytotoxic agent with PDT, and the properties of singlet oxygen are sensitive to the microenvironment surrounding the PS. The quantum yield, lifetime and diffusion distance of singlet oxygen will vary depending on whether it is generated by free PS in aqueous solution or PS encapsulated in micelles. Studies have shown longer $^1O_2$ lifetimes and improved $^1O_2$ generation when porphyrin-based PS is incorporated into micelle carriers [19], and that the produced $^1O_2$ in the micelle core can escape out of the core efficiently [20]. Moreover, the micelle formulation may protect PpIX from photobleaching by ROS and reacting with biomolecules directly. Another advantage of incorporating porphyrin-based PS agents into micelles includes the ability to prevent aggregation, which can interfere with PS efficacy and decrease the fluorescence of the PS dye. Previously, our lab reported the use of polymeric micelles for the delivery of imaging agents [21,22], and/or hydrophobic drugs [23,24] for cancer diagnostic or therapeutic applications. In this study, we describe the use of micelle carriers for the delivery of PpIX using a biocompatible and biodegradable block copolymer, poly(ethylene glycol)-*b*-poly(D,L-lactide) (PEG-PLA). A unique correlation of structure and

photophysical properties of PpIX/PEG-PLA micelles was discovered. The fluorescence efficiency, $^1O_2$ quantum yield and PDT efficacy in cancer cells were found to be highly dependent on the mode (i.e. physical encapsulation vs. covalent conjugation) and PpIX loading density. These results contribute to the fundamental understanding of the nanocarrier effect on the photophysical properties of PpIX-containing micelles, which will facilitate the implementation of these photosensitive nanoparticles for PDT treatment of cancer and other diseases.

2. Methods

2.1. Syntheses of PEG-PLA and PpIX-conjugated PEG-PLA (PEG-PLA-PpIX)

The PEG-PLA (molecular weights of PEG and PLA blocks are 5kD) copolymer was synthesized by ring-opening polymerization of D,L-lactide (Alfa Aesar, Ward Hill, MA) in dry toluene at 115 °C for 24 hrs using MeO-PEG-OH as a macroinitiator and $Sn(Oct)_2$ as a catalyst following a published procedure [25]. For PEG-PLA-PpIX synthesis, PpIX (0.1 mmol, Sigma-Aldrich) was first dissolved in 20 mL dry THF. Then PEG-PLA (1.2 g), dicyclohexylcarbodiimide (0.1 mmol) and N, N-dimethylaminopyridine were added under dry nitrogen and stirred at room temperature for 48 hrs. After reaction, white precipitate of dicyclohexylurea was filtered and the filtrate was concentrated by rotavap. The residual mixture was dialyzed in distilled water and lyophilized. UV-Vis analysis showed that 75% of PEG-PLA-OH end groups were conjugated with PpIX.

2.2. Micelle production and characterization

PpIX/PEG-PLA micelles were produced by a solvent evaporation method as previously reported [25]. Briefly, a proper amount of PEG-PLA and free PpIX or PEG-PLA-PpIX were first dissolved in THF with PpIX weight ratio varying from 0.04% to 4%. The mixture was added dropwise to distilled water under sonication and then allowed to evaporate overnight to remove THF. The resulting PpIX-micelles were purified by centrifugation dialysis (MW cutoff 100 kD) to remove free PpIX.

The PpIX-micelles were characterized by TEM for particle morphology and zeta sizer (Malvern NanoZS) for zeta potential and hydrodynamic diameters. The PpIX loading density was measured by dissolving a solid micelle sample in THF and quantified by UV-Vis analysis using a previously established calibration curve. The UV-Vis absorption spectra of PpIX-micelles were recorded at room temperature using a Shimadzu UV spectrophotometer (UV-1800), the emission spectra were obtained using a Hitachi fluorescence spectrophotometer (F-7000).

2.3. Singlet oxygen detection

The amount of $^1O_2$ was measured by following the loss of UV absorbance or emission [26] of ADPA in the aqueous PpIX-micelle solutions. Briefly, a series of air-saturated PpIX-micelle solutions (1 mL) were prepared with anthracene-9,10-dipropionic acid (ADPA, 10 μM) and fresh PpIX micelles. The solution was illuminated under a laser light (λ = 532 nm, power density = 10 mW/cm^2). The consumptions of ADPA (A_0-A_t, A_0 and A_t are the absorption of ADPA at 378nm before and after irradiation, respectively) were followed by monitoring its absorption decrease at 378 nm over time. Relative $^1O_2$ yields (Φ_Δ) were calculated by the slopes of the ADPA conversion and normalized to 0.2% PpIX-conjugated micelles.

2.4. PDT efficacy of PpIX-micelles in H2009 cells

H2009 human lung cancer cells were cultured in RPMI 1640 medium supplemented with 5% fetal bovine serum and antibiotics (Penicillin-Streptomycin) at 37 °C in a 10% CO_2

humidified incubator. One day before the PDT treatments, H2009 cells were trypsinized using 0.05% trypsin-EDTA and seeded (10,000 cells/well) into 48-well plates. Cell culture media were then replaced by media containing predetermined doses of PpIX micelles and incubated for 24 hrs. For the PDT study, cells were illuminated with laser (λ = 532 nm, power density = 20 mW/cm^2) for 10 mins. After irradiation, H2009 cells were allowed to grow for an additional 5 days in fresh media. Relative cell survival was measured by a DNA assay using Hoechst dye 33258 [27] and data were graphed as means of treated/control (T/C) ± SE X 100% from three independent experiments performed in sextuplicate. Dark toxicity was assessed from H2009 cells with PpIX-micelle incubation but without laser light exposure. Student's t-test was performed for statistical analysis (p value less than 0.05 is considered significant).

2.5. Confocal laser scanning microscopy of micelle uptake in H2009 cells

Confocal imaging studies were performed on a Nikon TE2000E confocal laser scanning microscope. H2009 cells were seeded in a glass-bottomed culture dish and allowed to attach overnight. The media were replaced with fresh media containing different PpIX-micelle samples at 100 μg/mL. H2009 cells were examined at different time points with a 600× total magnification (λ_{ex} = 405 nm, λ_{em} = 605±35 nm). ImageJ software (National Institutes of Health) was utilized to quantify the mean fluorescence intensity (MFI) of the PpIX-micelles *in vitro*.

3. Results

3.1. Production and physical characterization of PpIX-micelles

Two series of PpIX/PEG-PLA micelles were generated: one through a non-covalent hydrophobic encapsulation strategy and another via covalent conjugation of PpIX to the hydroxyl group of PEG-PLA through ester linkage (Fig. 1A). In both series, PpIX loading density (weight percentage of PpIX over micelles) was varied from 0.04% to 4%. Transmission electron microcopy (TEM) illustrated that PpIX-containing micelles had a spherical morphology (Fig. 1B). Dynamic light scattering (DLS) analysis showed that the micelle diameters were approximately 30 nm (Fig. 1C), with slight although statistically insignificant increase of micelle size with an increase in PpIX loading density (Table 1). Zeta potential (ξ) measurements showed that the micelle surface became more negatively charged with increased loading of PpIX in both series. For example, the ξ values decreased from -6.9 ± 1.5 to -13.3 ± 1.7 and -19.6 ± 1.3 mV for 0% (blank), 0.2% and 4% PpIX-encapsulated micelles, respectively (Table 1). A similar trend was also observed for PpIX-conjugated micelles. We attribute the decrease in ξ potential to the increased surface density of the negatively charged carboxylate (-COO$^-$) groups in higher PpIX-loading micelles.

3.2. UV-Vis and fluorescence properties of PpIX micelles

The UV-Vis absorption spectra of free PpIX monomer, dimer and aggregates are shown in Fig. 2A. In ethyl acetate (EA), PpIX stayed as a monomer with a sharp Soret band at 404 nm. At pH 11 in phosphate buffer, PpIX existed as a dimer and the Soret band blue shifted to 380 nm. At pH 7 in phosphate buffer, a greatly broadened split Soret band (maxima at 352 and 450 nm) of moderate intensity was observed, which correlates with the formation of extended aggregates in solution. In ethyl acetate, PpIX monomer showed bright fluorescence at 632 nm (λ_{ex} = 404 nm, Fig. 2B). For the PpIX dimer in an aqueous environment (pH 11), the fluorescence intensity decreased with a blue shift of emission peak (λ_{em} = 620 nm, λ_{ex} = 404 nm). For PpIX aggregates at pH 7, the fluorescence intensity became very weak (Fig. 2B).

The absorption spectra of PpIX-encapsulated micelles were highly dependent on the loading percentage of PpIX (Fig. 2C). Between 0.04% and 0.2% loading, PpIX existed mostly as a monomer in the micelle core as indicated by the Soret band at 404 nm. At 0.5%, a mixture of PpIX monomers and dimers was present. Above 1% in PpIX loading, PpIX formed aggregates in the micelle core as shown by the broadly split Soret bands. Fluorescence emission of PpIX-encapsulated micelles reached a maximum (λ_{em} = 630 nm) with 0.2% loading density. At higher loading density (>1%), the fluorescence intensity decreased dramatically (Fig. 2D), consistent with the formation of PpIX aggregates inside the micelle core. For PpIX-conjugated micelles, the absorption spectra showed that PpIX existed mostly as monomers between 0.04 and 0.2% PpIX loading density (Fig. 2E). At 0.2%, PpIX-conjugated micelles had a slightly higher fraction of PpIX in the monomeric state as indicated by the sharper Soret band (half-peak width was 63 nm) than 0.2% PpIX-encapsulated micelles (70 nm). At higher PpIX loading (i.e. 2% or 4%), PpIX existed mostly in the dimeric state as indicated by the blue-shifted Soret band. Similar to PpIX-encapsulated micelles, the fluorescence intensity of PpIX-conjugated micelles reached a maximum (λ_{em} = 630 nm) at 0.2% PpIX loading density and decreased significantly at higher PpIX loading (Fig. 2F). For both PpIX-conjugated and PpIX-encapsulated micelles, we chose 0.2% and 4% loading densities for the subsequent photophysical and PDT efficacy studies.

3.3. Efficiency of $^1O_2$ generation

The formation of $^1O_2$ was measured by the bleaching of ADPA dye, which was monitored by following the net loss of ADPA absorption at 378 nm over time (Fig. 3) [28,29]. The relative quantum yields (Φ_Δ) of $^1O_2$ generation from different micelle formulations were measured and listed in Table 1. The Φ_Δ values were normalized to 0.2% PpIX-conjugated micelles. At 0.2% PpIX loading density, PpIX-encapsulated micelles showed a smaller Φ_Δ (0.82) compared to PpIX-conjugated micelles (1.0). At 4% PpIX loading density, PpIX-conjugated micelles showed a much higher relative Φ_Δ value (0.48) than PpIX-encapsulated micelles (0.06). The Φ_Δ values correlate with the state of the PpIX inside the micelle cores (i.e. $\Phi_{\Delta,\,monomer} > \Phi_{\Delta,\,dimer} \gg \Phi_{\Delta,\,aggregates}$).

3.4. PDT efficacy in H2009 lung cancer cells

Fig. 4 shows the phototoxicity and dark toxicity of different PpIX-micelles in H2009 lung cancer cells after 24 hr incubation. For phototoxicity measurement, the cells were irradiated with laser light (λ=532 nm, power density = 20 mW/cm^2) for 10 mins. Cell cytotoxicity was measured as the percentage of the viable cells over the untreated cell control (i.e. without micelle incubation and laser exposure). For blank PEG-PLA micelles, the H2009 cells did not show any observable phototoxicity or dark toxicity (data not shown). For PpIX-micelles, several major observations can be made from the PDT data. First, the phototoxicities of 0.2% PpIX-micelles (either encapsulated or conjugated formulation) were significantly lower than those of 4% PpIX-micelles at the same micelle dose. For example, the IC_{50} (micelle concentration causing 50% toxicity) values were 51 ± 4 and 21 ± 2 μg/mL (p = 0.002) for 0.2% and 4% PpIX-encapsulated micelles, respectively. The difference was more pronounced in PpIX-conjugated micelles, as illustrated by 58 ± 3 and 3 ± 2 μg/mL (p = 0.0003) for 0.2% and 4% loading density, respectively. These data are contradictory to the $^1O_2$ results from the test tube studies where higher Φ_Δ values were observed for 0.2% PpIX-micelles. Second, 4% PpIX-encapsulated micelles showed significantly higher dark toxicity than the other micelle formulations. For example, an 80% relative survival was observed at a micelle dose of 8 ± 3 μg/mL; in contrast, none of the other PpIX-micelles showed similar dark toxicity even at the highest micelle dose of 80 μg/mL. Third, 4% PpIX-conjugated micelles demonstrated the largest PDT therapeutic window between the phototoxicity (Fig. 4B, red open circles) and dark toxicity (Fig. 4B, black solid circles).

Their phototoxicity was the highest among all micelles while the dark toxicity was comparable to 0.2% PpIX-micelles and much lower than 4% PpIX-encapsulated micelles (Fig. 4).

3.5. Intracellular fluorescence of PpIX-micelles

Confocal laser scanning microscopy was used to examine micelle uptake and PpIX release from different PpIX-micelles in H2009 cells over time. Both 0.2% PpIX-micelle formulations had similar fluorescence data; therefore only 0.2% PpIX-encapsulated micelles were shown (Fig. 5A). At 1 hr, the 0.2% PpIX-micelles showed similar intracellular fluorescence over the other two 4% PpIX-micelles. In addition, the fluorescence intensity from the 0.2% PpIX-micelles did not change considerably over the time course from 1 to 24 hrs (Fig. 5A and 5D black bars). In contrast, the 4% PpIX-encapsulated micelles (Fig. 5B and 5D red bars) showed a dramatic increase in fluorescence intensity in H2009 cells from 1 to 4 hrs (e.g. MFI values were 3.6 ± 1.1 and 20.7 ± 3.7 at 1 hr and 4 hrs, respectively; $p < 0.001$). The MFI values (20.7 ± 3.7 and 22.4 ± 3.8 at 4 and 24 hrs, respectively) remained relatively the same from 4 to 24 hrs ($p = 0.52$). Unlike the 4% PpIX-encapsulated micelles, the intracellular fluorescence intensity of H2009 cells incubated with 4% PpIX-conjugated micelles (Fig. 5C and 5D blue bars) showed a pattern of steady increase from 2.8 ± 0.4 at 1 hr to 15.8 ± 1.6 at 24 hrs ($p < 0.001$).

4. Discussion

The objective of the current study was to develop PpIX-micelles and investigate their photophyscial properties and PDT efficacy in cancer cells. PpIX is a potent photosensitizer and although its precursor, 5-ALA (Levulan®) has been clinically approved by the FDA, poor membrane permeability was a major limitating factor to achieve the desired clinical efficacy [7]. To overcome this limitation, we aimed to establish a micellar nanocarrier using a biocompatible and biodegradable PEG-PLA copolymer to directly deliver PpIX to cancer cells. Currently, Genexol™, a PEG-PLA micelle formulation for the delivery of paclitaxel, has already been clinically approved for cancer treatment in S. Korea [30].

PpIX is planar molecule with four conjugated pyrrole rings (Fig. 1) [31]. PpIX can easily aggregate in aqueous solution and its aggregation behavior has been extensively studied as a function of pH and ionic strength [32,33]. In the pH range of 0-3, PpIX stays as a monomer with a sharp Soret band at 404 nm and four Q-bands; at pH > 8, PpIX exists as a dimer with a sharp Soret band at 388 nm and four weak Q-bands; and in the pH range 3-7, PpIX forms extended aggregates with two splitting weak Soret bands centered at 350 and 460 nm and four weak Q bands. In these larger aggregates, porphyrins preferentially interact axially through π-π interactions and laterally by edge-to-edge hydrophobic interactions. Formation of intermolecular hydrogen bonds between the carboxylic acids was further hypothesized to contribute to the stabilization of the aggregated structures [32]. At physiological pH (7.4), PpIX has a very low aqueous solubility (~1 μg/mL) and cannot be directly administered intravenously.

Polymeric micelles provide an attractive nanocarrier option for the delivery of PpIX. In this study, we prepared PpIX-micelles by two different strategies: non-covalent encapsulation of PpIX in the hydrophobic cores of micelles and covalent conjugation of PpIX to the core-forming block of the PEG-PLA copolymer (Fig. 1A). We systematically examined the UV-Vis absorption, fluorescence emission, $^1O_2$ yield and PDT efficacy of different PpIX-micelles. At low PpIX loading density (i.e., <0.2%), PpIX mostly stayed in the monomeric state as indicated by the sharp Soret band at 404 nm, strong fluorescence intensity, and high $^1O_2$ yield regardless of incorporation strategies. At high PpIX loading density (i.e., 4%), however, the incorporation strategy had a dramatic effect on the PpIX state in the

micelles. In PpIX-encapsulated micelles, aggregated forms of PpIX were observed as indicated by the split Soret bands and complete quenching of fluorescence and $^1O_2$ generation ($\Phi_\Delta = 0.06$). In comparison, the 4% PpIX-conjugated micelles showed that PpIX were present as dimers with retaining of considerable $^1O_2$ generation capacity ($\Phi_\Delta = 0.48$). These results are consistent with the previous reports that only PpIX monomers and dimers can be photoexcited to triplet state thus allowing for the generation of $^1O_2$ [34,35].

Interestingly, $^1O_2$ generation efficiency from different PpIX-micelles did not correlate with their phototoxicity in H2009 lung cancer cells. Despite having much higher $^1O_2$ yields, the two 0.2% PpIX-micelles showed significantly lower phototoxicities compared to the 4% PpIX-micelles at the same micelle dose (Fig. 4). To investigate this discrepancy, we used confocal laser scanning microscopy to examine the micelle uptake and PpIX release in H2009 cells. For pegylated micelle nanoparticles, cell uptake occurs through fluidic phase endocytosis where nanoparticles are internalized via endosomes and distributed to other intracellular organelles (e.g. lysosome, Golgi) [36,37]. At 4% drug loading, both micelle formulations had very low fluorescence emissions in cell culture media due to PpIX quenching within the micelle core (Fig. 1). With 4% PpIX-encapsulated micelles, rapid increases in fluorescence in H2009 cells was observed in the first 4 hrs (Fig. 5). We attribute this increase to the release of free PpIX from intact micelles as well as from dissociation of micelles into PEG-PLA unimers and free PpIX, which may further bind to cytosolic proteins or membrane structures leading to further elevated fluorescence. For 4% PpIX-conjugated micelles, higher intracellular fluorescence intensity was also observed over those from 0.2% PpIX-micelles, suggesting the dissociation of some micelles into PEG-PLA-PpIX unimers. Similar micelle dissociation events were also observed following exposure to fluorogenic PEG-*b*-poly(ε-caprolactone) micelles under biological conditions [38,39]. In comparison, 4% conjugated micelles were more stable and had slower micelle dissociation kinetics compared to 4% encapsulated micelles in cell culture medium (Supplementary Fig. S1), which is consistent with the fast equilibrium for 4% PpIX-encapsulated micelles and steady increase for 4% conjugated micelles in intracellular fluorescence measurements.

Our data show that 4% PpIX-conjugated micelles provided the largest PDT therapeutic index compared to the other micelle formulations tested (Fig. 4). Several factors may contribute to this enhanced performance. First, conjugation of PpIX to the PLA segment prevented the formation of highly aggregated structures as in the 4% PpIX-encapsulated micelles. Consequently, the intact 4% PpIX-conjugated micelles had much higher $^1O_2$ yield ($\Phi_\Delta = 0.48$) than 4% PpIX-encapsulated micelles ($\Phi_\Delta = 0.06$). Second, it is known that high concentrations of free PpIX in cells can induce dark toxicity due to the binding of PpIX to mitochondrial membranes [40-42]. As such, PpIX conjugation to the PEG-PLA copolymer can effectively prevent the release of free PpIX and avoid dark toxicity. Third, 4% PpIX-conjugated micelles showed pattern of steady increase in intracellular fluorescence, which suggest uptake and the slow release of conjugated PpIX inside the cells for improved phototoxicity over time. The prolonged PpIX accumulation may reflect the slower micelle dissociation kinetics to release PEG-PLA-PpIX. In contrast, in 4% PpIX-encapsulated micelles, after an initial increase no changes in fluorescence intensity was observed from 4 to 24 hrs, which indicates the reaching of equilibrium between PpIX-micelle uptake, PpIX release, and the subsequent clearance of released free PpIX. Although 4% PpIX-encapsulated micelles had higher intracellular fluorescence over 4% PpIX-conjugated micelles in confocal studies, chemical extraction of PpIX from cells showed that PpIX-conjugated micelles had higher intracellular PpIX accumulation than that of encapsulated micelles (Supplementary Fig. S2). These results further verified the protection of PpIX and its photosensitive properties in conjugated micelle formulations, making 4% PpIX-conjugated micelles the best formulation for PDT efficacy. It is interesting to note that for anticancer drug delivery, it is imperative that intact drug molecules be released from

nanocarriers. In this study, release of free PpIX from 4% PpIX-encapsulated micelles caused undesirable dark toxicity, while 4% PpIX-conjugated micelles allowed for an effective dose accumulation and higher phototoxicity with reduced dark toxicity in H2009 cells.

5. Conclusions

This study systematically investigated several PEG-PLA micelle formulations for the delivery of PpIX, a precursor of heme biosynthesis and a potent PDT agent. Non-covalent encapsulation and covalent conjugation strategies were employed to incorporate PpIX into PEG-PLA micelle nanocarriers, which yielded monomeric, dimeric and aggregated forms of PpIX in the micelle core. Although 0.2% PpIX-micelles had higher fluorescence intensity and more efficient $^1O_2$ generation in aqueous solution, 4% PpIX-micelles resulted in brighter fluorescence and higher PDT efficacy in cancer cells as a result of PpIX release and micelle dissociation. Among all formulations, 4% PpIX-conjugated micelles provided the highest PDT efficacy with relatively low dark toxicity. These results contribute to the mechanistic understanding of the structure-property relationships of PpIX-micelles and establish an optimal micelle formulation (e.g. 4% PpIX-conjugated micelles) for subsequent *in vivo* evaluation in animals.

Supplementary Material

Refer to Web version on PubMed Central for supplementary material.

Acknowledgments

This research is supported by the National Cancer Institute to JG (R01CA122994 and R01CA129011) and DAB (R01CA102792) and BDS (5 UL1 RR024982-02-pilot award-PI-Packer). GH is supported by a Susan G. Komen foundation postdoctoral fellowship (PDF0707216). This is manuscript CSCN058 from the program in Cell Stress and Cancer Nanomedicine in the Simmons Comprehensive Cancer Center at the University of Texas Southwestern Medical Center at Dallas.

References

1. Dolmans DE, Fukumura D, Jain RK. Photodynamic therapy for cancer. Nat Rev Cancer. 2003; 3:380–387. [PubMed: 12724736]
2. Castano AP, Mroz P, Hamblin MR. Photodynamic therapy and anti-tumour immunity. Nat Rev Cancer. 2006; 6:535–545. [PubMed: 16794636]
3. Celli JP, Spring BQ, Rizvi I, Evans CL, Samkoe KS, Verma S, Pogue BW, Hasan T. Imaging and photodynamic therapy: mechanisms, monitoring, and optimization. Chem Rev. 2010; 110:2795–2838. [PubMed: 20353192]
4. Snyder JW, Skovsen E, Lambert JD, Ogilby PR. Subcellular, time-resolved studies of singlet oxygen in single cells. J Am Chem Soc. 2005; 127:14558–14559. [PubMed: 16231893]
5. Ricchelli F, Gobbo S, Moreno G, Salet C, Brancaleon L, Mazzini A. Photophysical properties of porphyrin planar aggregates in liposomes. Eur J Biochem. 1998; 253:760–765. [PubMed: 9654076]
6. Kennedy JC, Pottier RH, Pross DC. Photodynamic therapy with endogenous protoporphyrin IX: basic principles and present clinical experience. J Photochem Photobiol B. 1990; 6:143–148. [PubMed: 2121931]
7. Uehlinger P, Zellweger M, Wagnieres G, Juillerat-Jeanneret L, van den Bergh H, Lange N. 5-Aminolevulinic acid and its derivatives: physical chemical properties and protoporphyrin IX formation in cultured cells. J Photochem Photobiol B. 2000; 54:72–80. [PubMed: 10739146]
8. Eleouet S, Rousset N, Carre J, Bourre L, Vonarx V, Lajat Y, Beijersbergen van Henegouwen GM, Patrice T. In vitro fluorescence, toxicity and phototoxicity induced by delta-aminolevulinic acid (ALA) or ALA-esters. Photochem Photobiol. 2000; 71:447–454. [PubMed: 10824596]
9. Fernandez JM, Bilgin MD, Grossweiner LI. Singlet oxygen generation by photodynamic agents. Journal of Photochemistry and Photobiology B: Biology. 1997; 37:131–140.

10. Chen W, Zhang J. Using nanoparticles to enable simultaneous radiation and photodynamic therapies for cancer treatment. J Nanosci Nanotechno. 2006; 6:1159–1166.
11. Lassalle HP, Dumas D, Gräfe S, D'Hallewin MA, Guillemin F, Bezdetnaya L. Correlation between in vivo pharmacokinetics, intratumoral distribution and photodynamic efficiency of liposomal mTHPC. J Controlled Release. 2009; 134:118–124.
12. Johansson A, Svensson J, Bendsoe N, Svanberg K, Alexandratou E, Kyriazi M, Yova D, Grafe S, Trebst T, Andersson-Engels S. Fluorescence and absorption assessment of a lipid mTHPC formulation following topical application in a non-melanotic skin tumor model. J Biomed Opt. 2007; 12:034026. [PubMed: 17614734]
13. Battah S, Balaratnam S, Casas A, O'Neill S, Edwards C, Batlle A, Dobbin P, MacRobert AJ. Macromolecular delivery of 5-aminolaevulinic acid for photodynamic therapy using dendrimer conjugates. Molecular Cancer Therapeutics. 2007; 6:876–885. [PubMed: 17363482]
14. Li Y, Jang WD, Nishiyama N, Kishimura A, Kawauchi S, Morimoto Y, Miake S, Yamashita T, Kikuchi M, Aida T, Kataoka K. Dendrimer generation effects on photodynamic efficacy of dendrimer porphyrins and dendrimer-loaded supramolecular nanocarriers. Chem Mater. 2007; 19:5557–5562.
15. Rossi LM, Silva PR, Vono LLR, Fernandes AU, Tada DB, Baptista McS. Protoporphyrin IX nanoparticle carrier: preparation, optical properties, and singlet oxygen generation. Langmuir. 2008; 24:12534–12538. [PubMed: 18834155]
16. Khdair A, Gerard B, Handa H, Mao G, Shekhar MP, Panyam J. Surfactant-polymer nanoparticles enhance the effectiveness of anticancer photodynamic therapy. Mol Pharm. 2008; 5:795–807. [PubMed: 18646775]
17. Rijcken CJ, Hofman JW, van Zeeland F, Hennink WE, van Nostrum CF. Photosensitiser-loaded biodegradable polymeric micelles: preparation, characterisation and in vitro PDT efficacy. J Control Release. 2007; 124:144–153. [PubMed: 17936395]
18. Master AM, Rodriguez ME, Kenney ME, Oleinick NL, Gupta AS. Delivery of the photosensitizer Pc 4 in PEG-PCL micelles for in vitro PDT studies. J Pharm Sci. 2010; 99:2386–2398. [PubMed: 19967780]
19. Li B, Moriyama EH, Li F, Jarvi MT, Allen C, Wilson BC. Diblock copolymer micelles deliver hydrophobic protoporphyrin IX for photodynamic therapy. Photochem Photobiol. 2007; 83:1505–1512. [PubMed: 18028227]
20. Lindig BA, Rodgers MAJ, Schaap AP. Determination of the lifetime of singlet oxygen in D_2O using 9,10-anthracenedipropionic acid, a water-soluble probe. J Am Chem Soc. 1980; 102:5590–5593.
21. Ai H, Flask C, Weinberg B, Shuai X, Pagel MD, Farrell D, Duerk J, Gao JM. Magnetite-loaded polymeric micelles as ultrasensitive magnetic-resonance probes. Adv Mater. 2005; 17:1949–1952.
22. Khemtong C, Kessinger CW, Ren JM, Bey EA, Yang SG, Guthi JS, Boothman DA, Sherry AD, Gao JM. In vivo Off-resonance saturation magnetic resonance imaging of alpha(v)beta(3)-targeted superparamagnetic nanoparticies. Cancer Research. 2009; 69:1651–1658. [PubMed: 19190328]
23. Nasongkla N, Bey E, Ren JM, Ai H, Khemtong C, Guthi JS, Chin SF, Sherry AD, Boothman DA, Gao JM. Multifunctional polymeric micelles as cancer-targeted, MRI-ultrasensitive drug delivery systems. Nano Lett. 2006; 6:2427–2430. [PubMed: 17090068]
24. Nasongkla N, Shuai X, Ai H, Weinberg BD, Pink J, Boothman DA, Gao JM. cRGD-functionalized polymer micelles for targeted doxorubicin delivery. Angew Chem Int Edit. 2004; 43:6323–6327.
25. Shuai X, Ai H, Nasongkla N, Kim S, Gao J. Micellar carriers based on block copolymers of poly(epsilon-caprolactone) and poly(ethylene glycol) for doxorubicin delivery. J Control Release. 2004; 98:415–426. [PubMed: 15312997]
26. Liu YF, Chen W, Wang SP, Joly AG. Investigation of water-soluble x-ray luminescence nanoparticles for photodynamic activation. Appl Phys Lett. 2008; 92
27. Labarca C, Paigen K. A simple, rapid, and sensitive DNA assay procedure. Anal Biochem. 1980; 102:344–352. [PubMed: 6158890]
28. Oar MA, Serin JA, Dichtel WR, Frechet JMJ. Photosensitization of singlet oxygen via two-photon-excited fluorescence resonance energy transfer in a water-soluble dendrimer. Chem Mater. 2005; 17:2267–2275.

29. Ding HY, Wang XS, Song LQ, Chen JR, Yu JH, Chao-Li, Zhang BW. Aryl-modified ruthenium bis(terpyridine) complexes: Quantum yield of $^1O_2$ generation and photocleavage on DNA. J Photoch Photobio A. 2006; 177:286–294.
30. Kim DW, Kim SY, Kim HK, Kim SW, Shin SW, Kim JS, Park K, Lee MY, Heo DS. Multicenter phase II trial of Genexol-PM, a novel Cremophor-free, polymeric micelle formulation of paclitaxel, with cisplatin in patients with advanced non-small-cell lung cancer. Ann Oncol. 2007; 18:2009–2014. [PubMed: 17785767]
31. Caughey WS, Ibers JA. Crystal and molecular structure of the free base porphyrin, protoporphyrin IX dimethyl ester. J Am Chem Soc. 1977; 99:6639–6645. [PubMed: 19518]
32. Scolaro LM, Castriciano M, Romeo A, Patane S, Cefali E, Allegrini M. Aggregation Behavior of Protoporphyrin IX in Aqueous Solutions: Clear Evidence of Vesicle Formation. The Journal of Physical Chemistry B. 2002; 106:2453–2459.
33. Maiti NC, Mazumdar S, Periasamy N. Dynamics of Porphyrin Molecules in Micelles - picosecond time-resolved fluorescence anisotropy studies. J Phys Chem. 1995; 99:10708–10715.
34. Craw M, Redmond R, Truscott TG. Laser flash-photolysis of hematoporphyrins in some homogeneous and heterogeneous environments. J Chem Soc Farad T 1. 1984; 80:2293–2299.
35. Ricchelli F. Photophysical properties of porphyrins in biological membranes. J Photochem Photobiol B. 1995; 29:109–118. [PubMed: 7472807]
36. Allen C, Yu Y, Eisenberg A, Maysinger D. Cellular internalization of PCL_{20}-b-PEO_{44} block copolymer micelles. Biochim Biophys Acta. 1999; 1421:32–38. [PubMed: 10561469]
37. Mukherjee S, Ghosh RN, Maxfield FR. Endocytosis. Physiol Rev. 1997; 77:759–803. [PubMed: 9234965]
38. Chen H, Kim S, He W, Wang H, Low PS, Park K, Cheng JX. Fast release of lipophilic agents from circulating PEG-PDLLA micelles revealed by in vivo forster resonance energy transfer imaging. Langmuir. 2008; 24:5213–5217. [PubMed: 18257595]
39. Savic R, Azzam T, Eisenberg A, Maysinger D. Assessment of the integrity of poly(caprolactone)-*b*-poly(ethylene oxide) micelles under biological conditions: a fluorogenic-based approach. Langmuir. 2006; 22:3570–3578. [PubMed: 16584228]
40. Braverman S, Helson C, Helson L. Hemin toxicity in a human epithelioid sarcoma cell line. Anticancer Res. 1995; 15:1963–1967. [PubMed: 8572585]
41. Goldstein L, Teng ZP, Zeserson E, Patel M, Regan RF. Hemin induces an iron-dependent, oxidative injury to human neuron-like cells. J Neurosci Res. 2003; 73:113–121. [PubMed: 12815715]
42. Sandberg S. Protoporphyrin-induced photodamage to mitochondria and lysosomes from rat liver. Clin Chim Acta. 1981; 111:55–60. [PubMed: 7226541]

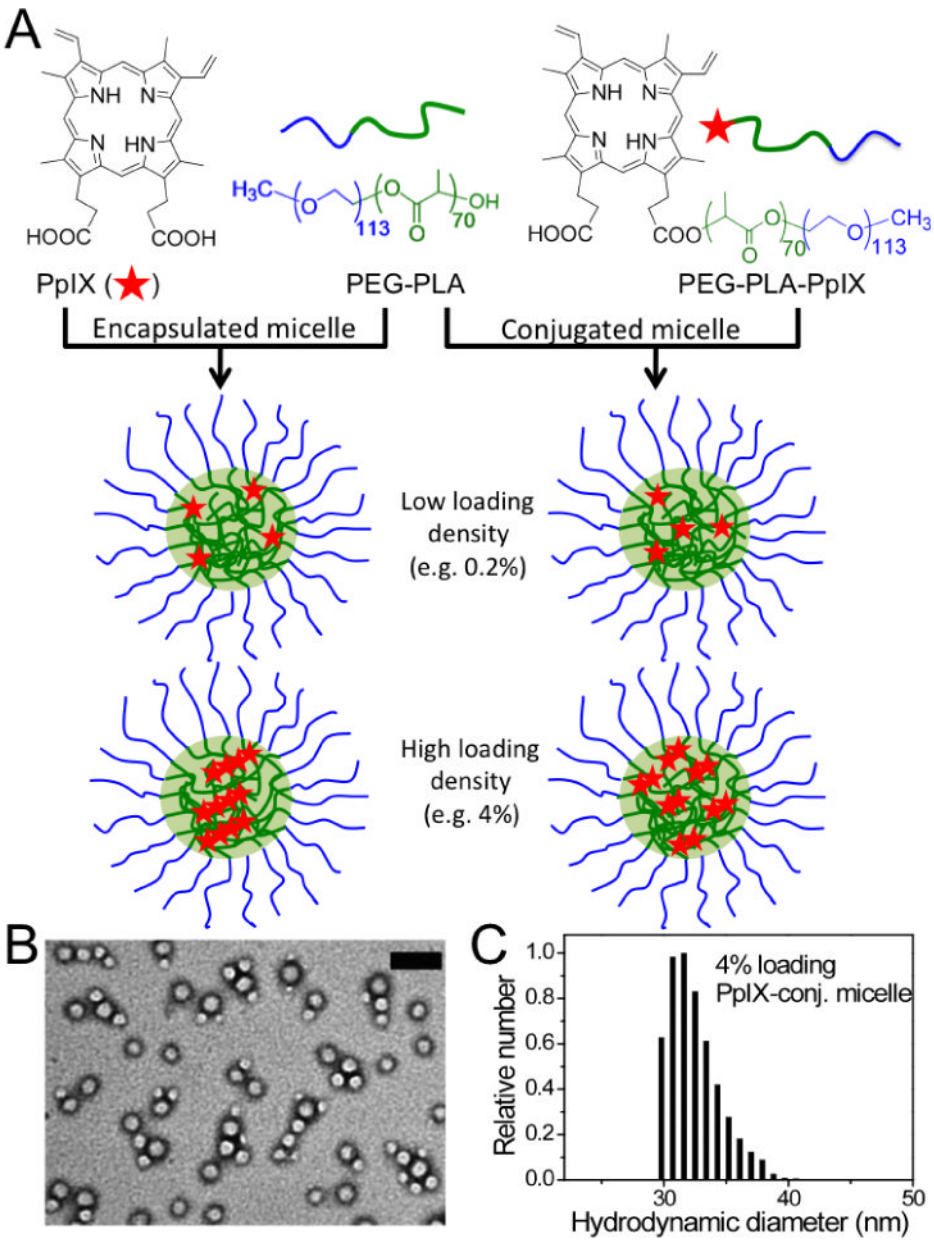

Fig. 1.

(A) Schematic illustration of two different types of PpIX/PEG-PLA micelles from non-covalent encapsulation and covalent conjugation methods. At low loading density (i.e. 0.2%), PpIX exists as monomers in both micelle formulations; at high loading density (i.e. 4%), PpIX is present as aggregates or dimers in encapsulated and conjugated micelles, respectively. (B) A representative transmission electron microscopy (TEM) image of 4% PpIX-conjugated micelles counter-stained with 2% PTA. The scale bar is 100 nm. (C) Histogram depicting hydrodynamic size distribution of 4% PpIX-conjugated micelles by dynamic light scattering (DLS).

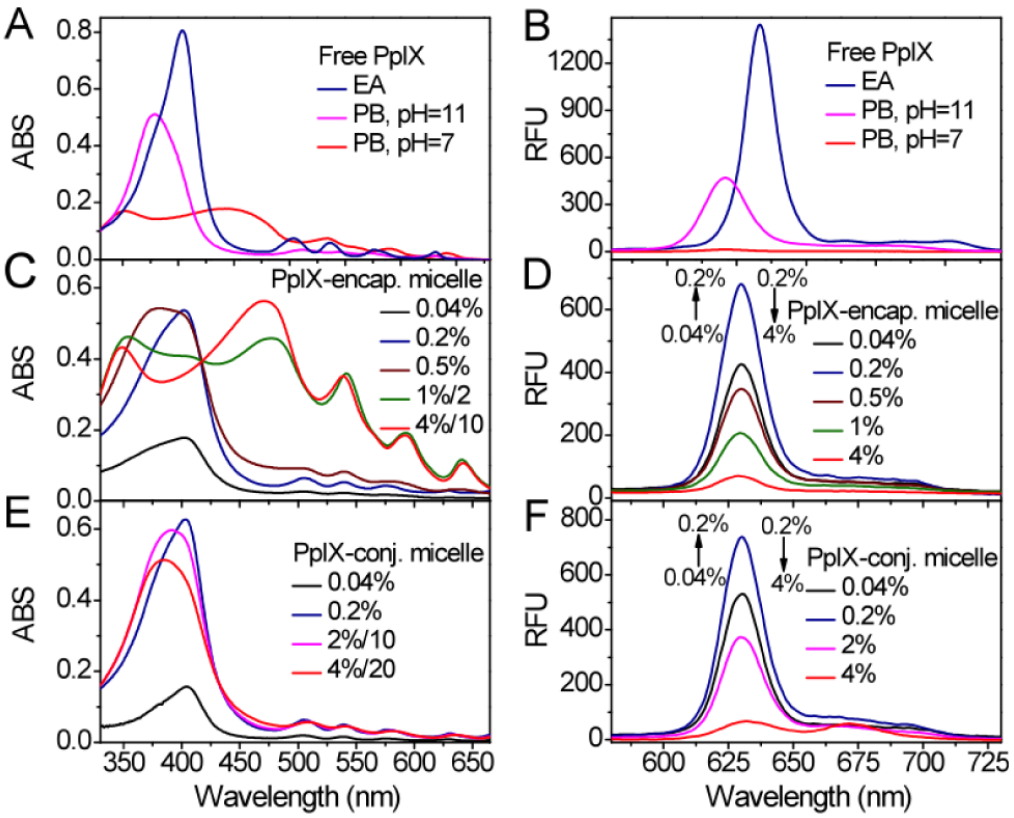

Fig. 2.

UV-Vis absorption (A,C,E) and fluorescence (B,D,F, λ_{ex} = 404 nm) spectra of free PpIX, PpIX-encapsulated micelles, and PpIX-conjugated micelles, respectively. Free PpIX (A,B) existed as monomers in ethyl acetate (EA), dimers in phosphate buffer (PB) at pH = 11, and aggregates in phosphate buffer (PB) at pH = 7 ([PpIX] = 8 μM in all samples). PpIX-encapsulated micelles (C,D) show PpIX existed as monomers at low loading density (<0.2%) and as aggregates at high loading density (>1%). In comparison, PpIX-conjugated micelles (E,F) showed that PpIX existed as monomers at low loading density (<0.2%) and as dimers at high loading density (>2%). All the micelles were measured at 2 mg/mL concentration except for those indicated by a dilution factor in C and E for higher loading PpIX-micelles.

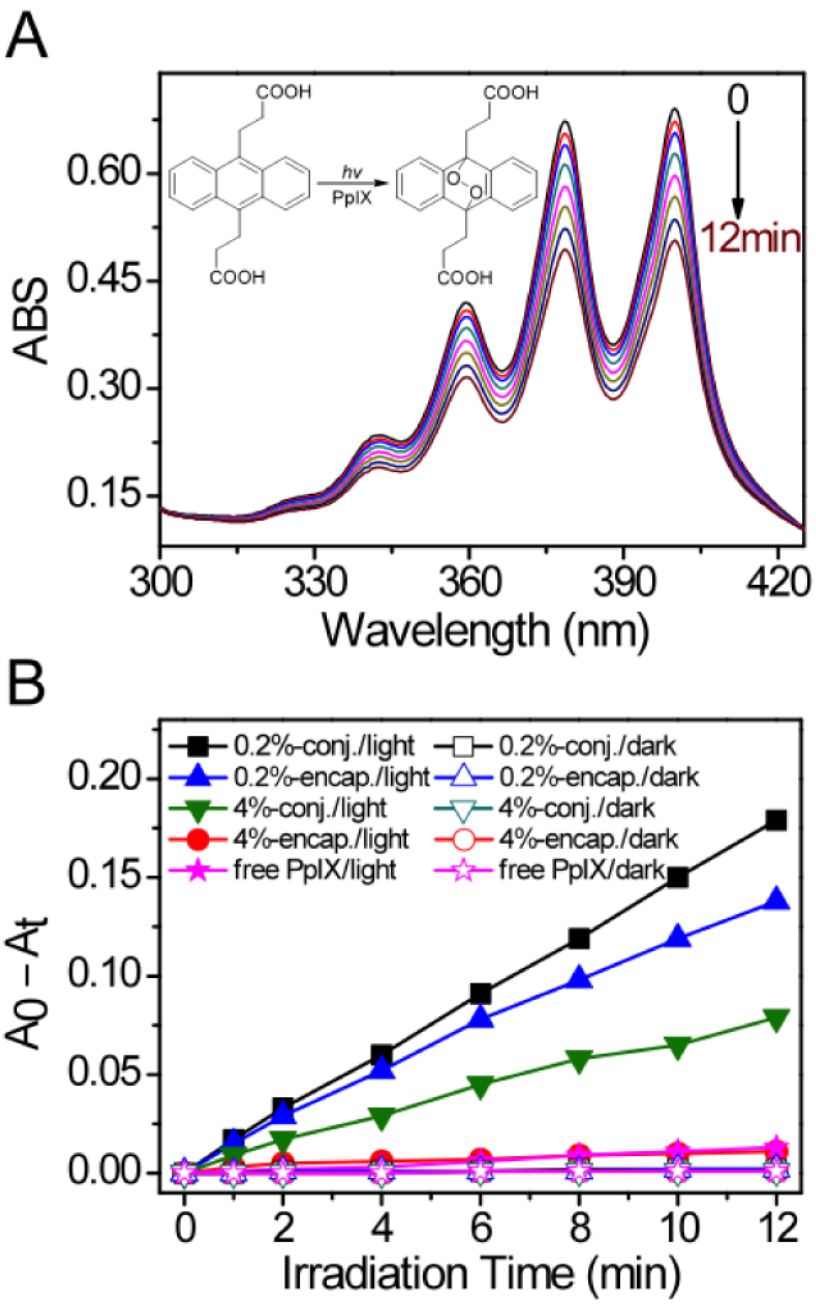

Fig. 3.

(A) Exemplar UV-Vis spectra of ADPA in the presence of 0.2% PpIX-conjugated micelles as a function of laser irradiation time (λ = 532 nm, power density = 10 mW/cm^2). Inset figure shows the reaction of ADPA with $^1O_2$. (B) ADPA consumption over time in solutions containing different PpIX-micelles with (solid symbols) and without laser irradiation (open symbols). A_0 and A_t are absorption of ADPA at 378 nm before and after irradiation, respectively.

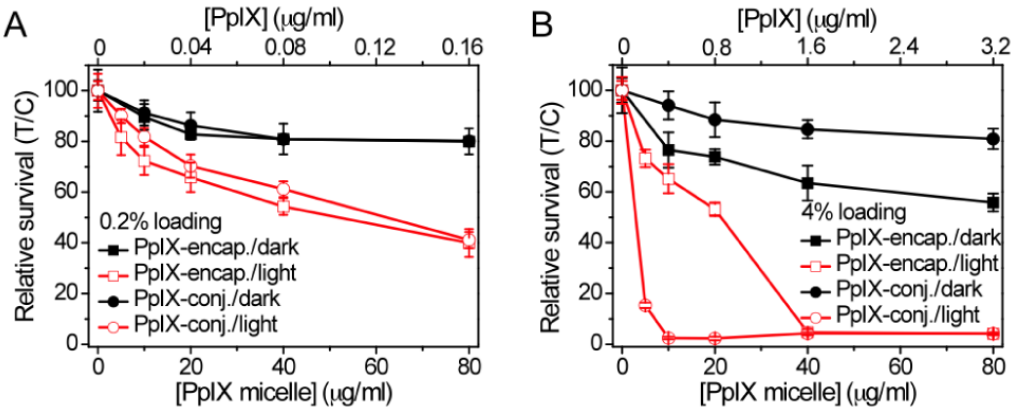

Fig. 4.

Phototoxicity (red open symbols) and dark-toxicity (black solid symbols) of (A) 0.2% PpIX-micelles and (B) 4% PpIX-micelles as a function of micelle/PpIX dose after 24 hr incubation. The relative survival were normalized to the control cells without light nor PpIX. Both PpIX-encapsulated and PpIX-conjugated formulations were shown in each figure. Laser irradiation conditions were: $\lambda = 532$ nm, power density = 20 mW/cm^2, total light dose = 12 J/cm^2.

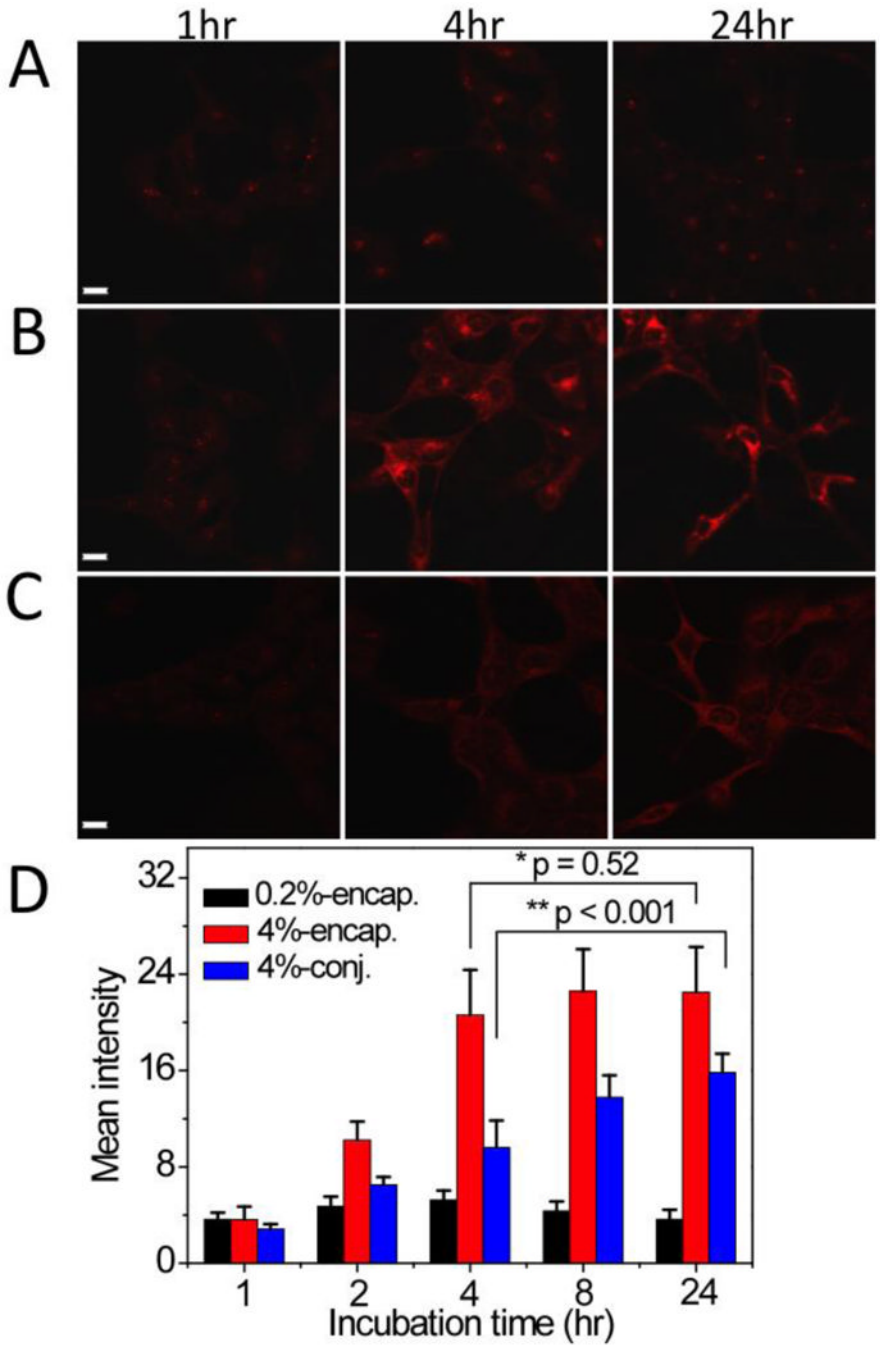

Fig. 5.

Confocal laser scanning microscopy images of H2009 lung cancer cells incubated with PpIX-micelles over time. (A) 0.2% PpIX-encapsulated micelles; (B) 4% PpIX-encapsulated micelles; and (C) 4% PpIX-conjugated micelles. Red fluorescence is from structural moieties containing PpIX. All micelle concentrations were maintained at 100 μg/mL. The scale bars are 20 μm in A-C. (D) The mean fluorescence intensity from 10 cells as a function of incubation time for different PpIX-micelles. The p values were calculated using the Student's t-test and indicated in D between paired groups of comparison.

Table 1

Comparison of the physical properties of free PpIX and PpIX/PEG-PLA micelles.

PpIX samples	PpIX loading (wt%)[a]	Diameter (nm)[b]	ξ (mV)	Soret band (nm)	Q-bands (nm)	Emission (nm)	Φ_Δ[c]
Free PpIX[d]	–	–	–	352, 450	535, 562, 589, 642	620	0.05
PEG-PLA micelles	–	31±5	-6.9±1.5	–	–	–	–
PpIX-encapsulated	0.2 %	30±6	-13.3±1.7	404	506, 538, 574, 629	630	0.82
micelles	4%	33±6	-19.6±1.3	348, 472	542, 565, 593, 640	630	0.06
PpIX-conjugated	0.2%	30±6	-7.4±1.1	403	506, 538, 575, 630	630	1.0
micelles	4%	32±6	-20.8±1.6	385	510, 542, 581, 635	632, 672	0.48

[a] PpIX loading density was measured as the weight of PpIX over that of total micelles.

[b] By dynamic light scattering.

[c] Relative $^1O_2$ yields that were normalized to that of 0.2% PpIX-conjugated micelles.

[d] PpIX at 2 μM in phosphate buffer (PB) at pH 7 (aggregated state).